NASA TECHNICAL NOTE

NASA TN D-6863

APOLLO 9 THERMAL-CONTROL-COATING DEGRADATION

by James A. Smith
Manned Spacecraft Center
Houston, Texas 77058

NATIONAL AERONAUTICS AND SPACE ADMINISTRATION • WASHINGTON, D. C. • JUNE 1972

1. Report No.	2. Government Accession No.	3. Recipient's Catalog No.
NASA TN D-6863		

4. Title and Subtitle	5. Report Date
APOLLO 9 THERMAL-CONTROL-COATING DEGRADATION	June 1972
	6. Performing Organization Code

7. Author(s)	8. Performing Organization Report No.
James A. Smith, MSC	MSC S-314
	10. Work Unit No.
9. Performing Organization Name and Address	914-11-00-00-72
Manned Spacecraft Center Houston, Texas 77058	11. Contract or Grant No.
	13. Type of Report and Period Covered
12. Sponsoring Agency Name and Address	Technical Note
National Aeronautics and Space Administration Washington, D.C. 20546	14. Sponsoring Agency Code

15. Supplementary Notes

The MSC Director waived the use of the International System of Units (SI) for this Technical Note because, in his judgment, use of SI Units would impair the usefulness of the report or result in excessive cost.

16. Abstract

Analytical studies, ground-test data, and flight data before 1967 indicated that degradation of Apollo thermal-control coatings could be expected, possibly to an extent requiring spacecraft design changes to accomplish the worst-case lunar-landing mission. On the Apollo 9 mission, specimens of Apollo thermal-control coatings were retrieved by the astronauts during the extravehicular activity. These specimens were the first to be returned to earth from space unaffected by entry conditions. Subsequent measurements of the thermophysical properties (solar absorptance and hemispherical emittance) of the thermal-control-sample coatings revealed degradation levels well within the design capability of the Apollo spacecraft.

17. Key Words (Suggested by Author(s))	18. Distribution Statement
* Apollo 9 Mission * Thermal-Control-Coating Degradation * Inflight Thermal-Control-Coating Degradation	

19. Security Classif. (of this report)	20. Security Classif. (of this page)	21. No. of Pages	22. Price
None	None	18	$3.00

* For sale by the National Technical Information Service, Springfield, Virginia 22151

APOLLO 9 THERMAL-CONTROL-COATING DEGRADATION

By James A. Smith
Manned Spacecraft Center

SUMMARY

Degradation to thermal-control surfaces of the Apollo spacecraft became a major concern for accomplishing the lunar-landing missions. Ground and unmanned-flight test data were either not applicable or subject to uncertainty for use in performance analyses of Apollo subsystems. The use of protective covers was deemed unacceptable because of added weight and operational complexity. Analyses of some subsystem thermal performance showed that the lunar-landing-mission success depended on the extent of thermal-control-coating degradation.

The Apollo 9 mission was chosen to perform inflight retrieval of thermal-control-coating specimens exposed to the combined degradation sources of the Apollo mission environment. Also, this mission was chosen because it was the only mission before the first manned lunar landing in which extravehicular activities were planned.

No attempt was made to determine degradation levels from particular contamination sources, because the complexity of doing so was more than could be accommodated during one period of extravehicular activity. Results of the Apollo 9 thermal-control-coating degradation test showed that the total degradation was well within that required for the Apollo spacecraft subsystems to perform the lunar-landing mission.

INTRODUCTION

The Apollo spacecraft design uses thermal-control coatings for active and passive thermal control. The thermal-control coatings on the exterior of the Apollo spacecraft are exposed to contamination by plume impingement from the launch vehicle stage retrorockets and from the reaction control system (RCS) engine, boost heating effects, outgassing of ablative materials, and pyrotechnic discharge products. Analyses of some subsystem thermal performances showed that the success of the lunar-landing mission depended on the extent of thermal-control-coating degradation that could not be quantified by existing ground- and flight-test data. Thermal-control-coating samples retrieved in flight and returned to earth for evaluation would provide the necessary data to determine if the Apollo spacecraft design performance was adequate. The Apollo 9 mission was chosen to perform these inflight retrieval tasks, because it was the only mission before the first manned lunar landing in which extravehicular activities were planned.

This report provides a description of the thermal-control-coating samples, the locations on the spacecraft, and the method of sample retrieval. Preflight and postflight measurement procedures are discussed, and results of the thermophysical-property degradation of the material are presented. The Apollo 9 thermal-control-coating samples were exposed to representative lunar-mission environment contamination levels. Total degradation to the thermophysical properties of the thermal-control-coating samples confirmed that the Apollo spacecraft subsystems design was capable of fulfilling the requirements of the lunar-landing mission.

BACKGROUND

The Apollo command module (CM) and service module (SM) are subjected to a more severe boost environment than that encountered in Project Mercury or in the Gemini Program. Higher heating rates during the boost phase required thermal protection to the exposed CM ablator and to the SM outer shell. A jettisonable cork cover over the CM and cork bonded to the SM provide this protection.

The major sources of contamination that could cause degradation to the Apollo thermal-control coatings are as follows.

1. Carbon particles and decomposition gases produced by CM cork-cover ablation during ascent

2. Carbon particles and decomposition gases produced by SM cork ablation during ascent and during SM RCS engine firings

3. Solid rocket-motor products of combustion during staging of the launch escape system and boost vehicles

4. Exhaust products of combustion from the SM RCS hypergolic engines

5. Particle and combustion-products impingement from pyrotechnic separation devices

Each of the sources of contamination was evaluated separately to predict the maximum degradation to thermal-control coatings. However, analytical and test data sources used for the predictions were not directly applicable, were subject to large uncertainties because of experimental inaccuracies, or were highly questionable because of scaling factors or nonrepresentative environmental conditions. Obviously, a larger uncertainty exists for the predicted cumulative degradation.

Analyses of some spacecraft subsystems for the predicted values of thermal-control-coating degradation showed that marginally acceptable performance could be expected for worst-case lunar-landing missions. As a result of the uncertainty in predicting degradation and as a major program effort to design protection from the contaminants, an inflight experiment was planned to determine thermal-control-coating degradation. The Apollo 9 mission was chosen for the performance of this experiment because thermal-control-coating samples could be retrieved during the planned extravehicular activity (EVA). Because the Apollo 9 mission was earth orbital, the

spacecraft thermal-control coating could accept higher levels of degradation than lunar-landing missions without jeopardizing mission success.

THERMAL-CONTROL-COATING SAMPLE DESCRIPTION

Two types of thermal-control-coating samples were designed for the Apollo 9 mission: one for attachment to the SM and the other for attachment to the CM as shown in figure 1. The CM type of sample was also used on the lunar module (LM). The SM samples were designed to wedge over a Teflon mounting plate attached to the SM. The sample was closed by spring load about the swivel pin so that, when the sample was removed, the two thermal-control-coating surfaces would close facing each other to provide protection from inadvertent damage or smudging. The three SM samples were tethered together by a cable latched to the SM surface by clips to keep the cable in tension during the boost phase and to prevent vibration damage. Metal tabs were provided at the bottom of the Teflon mounting plates to restrain the sample from vibration during the boost phase. The CM and LM samples were also a hinged design to protect the thermal-control surfaces. A hole in the sampleholder allowed transmittance measurement of the window specimen without the removal of the specimen. To prevent damage to the LM outer surface, fiber-glass retainer clips were provided for the LM sample to restrain vibration of the release rings during the boost phase. On the CM sample, the space between the CM surface and the boost protective cover (BPC) prevented ring excursion from causing damage.

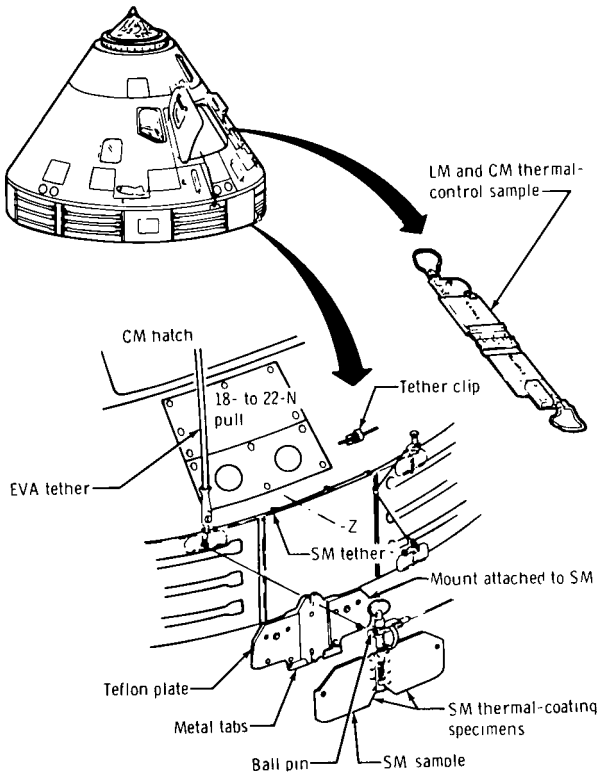

Figure 1. - Locations of thermal-control sampleholders on the CM and SM.

A sample-return container was designed to provide stowage for return of the samples. This container (fig. 2) had three slots with internal tension springs for the three SM samples and two slots with internal tension springs for the CM and LM samples. The lid and mounting flange incorporated a labyrinth seal, but no provisions were made to retain a vacuum in the container.

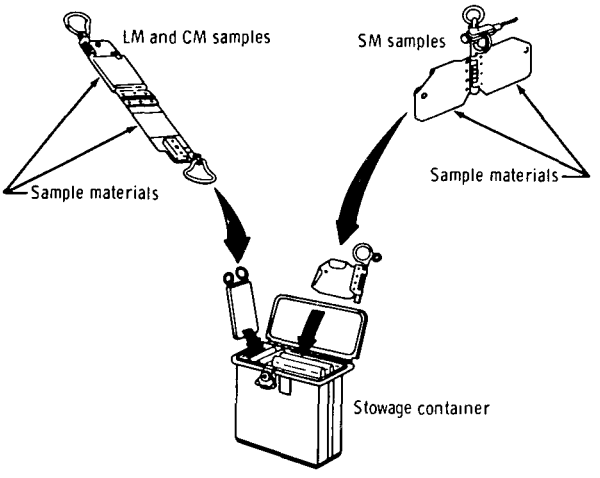

Figure 2. - Configuration of samples and sample container.

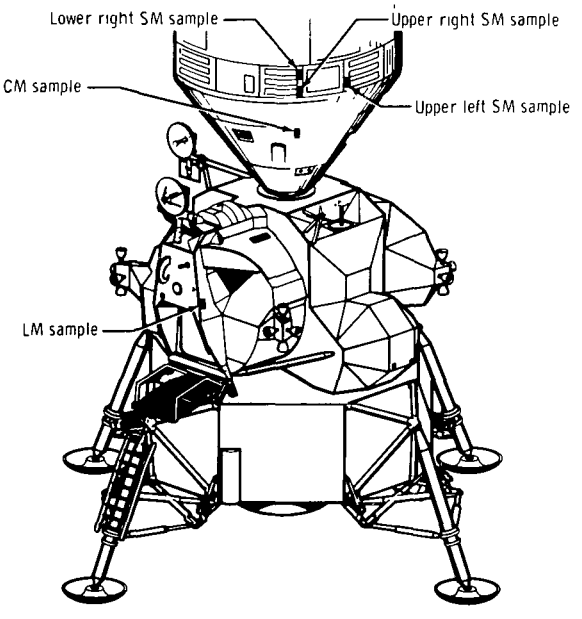

Figure 3. - Locations of thermal-control samples on the SM, CM, and LM.

THERMAL-CONTROL-SAMPLE LOCATIONS

The thermal-control-sample locations were established to obtain maximum degradation from the expected sources, to determine which source provided the maximum degradation, and to facilitate retrieval. A composite sketch (fig. 3) shows the sample locations and relative geometry to the RCS engines. The SM samples were located on the SM-to-CM fairing closeout structure and on the electrical power system (EPS) radiators (figs. 1 and 4). The upper left sample was alined with and approximately 1 meter forward of the minus X-axis translation RCS engine. This location was chosen to provide a maximum contamination effect from the RCS exhaust products. The upper right and lower right samples were located 104 centimeters circumferentially from the minus X-axis translation RCS engine. The upper right sample was horizontally alined with the upper left sample, and the lower right sample was 47 centimeters directly below the upper right sample. The sample locations were chosen to evaluate the effects of deposited charred cork from the BPC during boost.

The CM sample location, just outside the hatch (figs. 1 and 5), provided maximum effect of contamination from the tower jettison motors, which have a trajectory resulting in plume impingement on the CM hatch and window. The LM sample was located on the right side of the LM forward hatch primarily for ease of retrieval but also for determination of the potential degradation resulting from the SM-to-LM adapter pyrotechnic separation system.

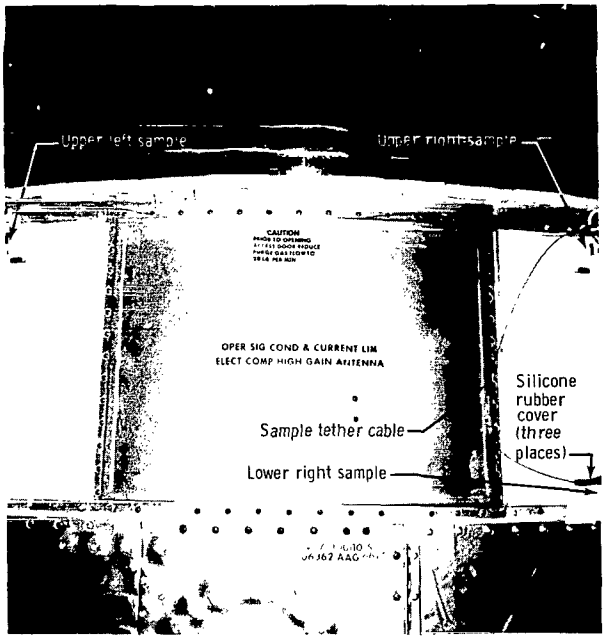

Figure 4. - Preflight installation of the SM thermal samples and tether.

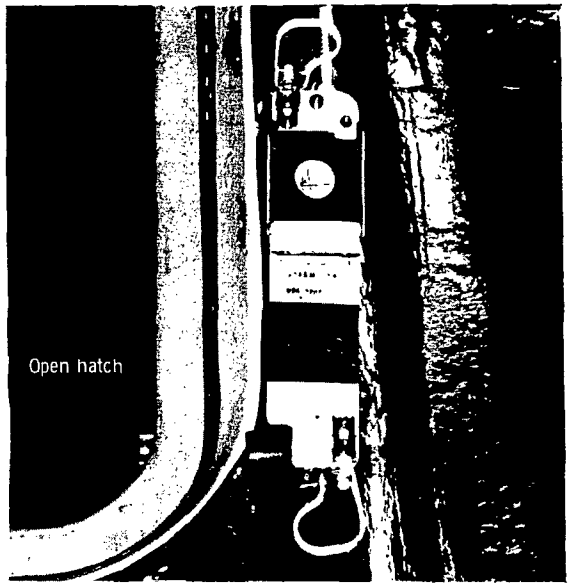

Figure 5. - Preflight installation of the CM thermal sample.

THERMAL-CONTROL-COATING MATERIALS

Each of the three SM samples was prepared with identical thermal-control coatings. The left-hand plate was prepared with a commercially available titanium dioxide-silicone base white paint that is used on the outboard surface of the SM panel covering the EPS fuel-cell bay. The right-hand plate was prepared with another commercially available zinc oxide-potassium silicate white paint that is used on the EPS radiator panels and on the environmental control system radiator panels.

One side of the CM sample contained a specimen of oxidized silicone monoxide over vacuum-deposited aluminum on a polyimide film substrate that was also used on the CM ablator outer surface. The other side of the CM sample contained a specimen of quartz glass, which is used in the outer pane of the CM windows. The LM sample contained a specimen of LM outer-window material and a specimen of anodized aluminum identical to many of the external LM surface panels.

THERMAL-CONTROL-SAMPLE RETRIEVAL

On March 6, 1969, approximately 73 hours after lift-off, the CM pilot opened the CM hatch and retrieved the SM samples (fig. 6). The CM sample was not in place; furthermore, no definite explanation for its disappearance is known. The LM pilot performed an intravehicular transfer to the LM and exited through the LM hatch. After

photography was accomplished, he retrieved the LM sample (fig. 7) and handed it to the spacecraft commander for subsequent intravehicular transfer to the CM. The samples were stowed for return to the Manned Spacecraft Center (MSC) where they were placed in bonded storage.

Figure 6. - Retrieval of the SM thermal samples by the CM pilot.

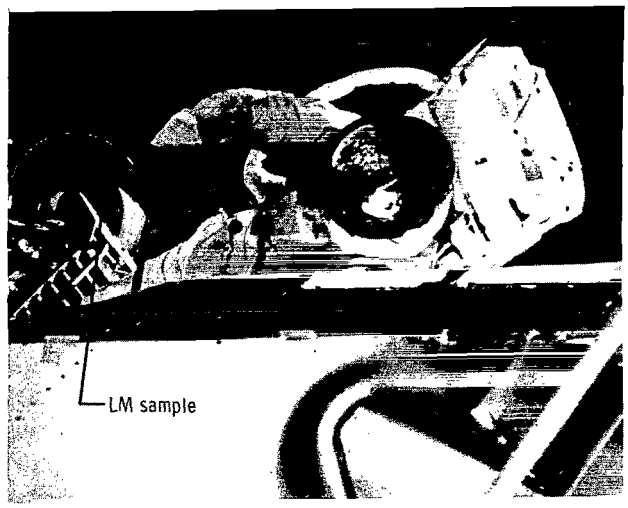

Figure 7. - Retrieval of the LM thermal sample by the LM pilot.

MEASUREMENTS OF FLIGHT SAMPLES

Preflight and Postflight Measurements

All flight articles were cleaned at the MSC and bagged before shipment to a support contractor for preflight measurements. After return to the MSC, the flight articles were again cleaned before shipment to the Kennedy Space Center for final installation on the spacecraft. Preflight measurements were accomplished by performing relative measurements on the flight samples (glass specimens excepted) because the size prohibited installation in the absolute-measuring devices. Absolute measurements of reference samples of the same material (as the flight-article thermal-control coatings) were used as standards. The properties of the flight samples were then determined by a spectral comparison of the absolute reflectance of the standard with the relative reflectance of the flight sample.

Postflight measurements were accomplished in the same manner as preflight measurements by using the relative-measurement procedure; additional absolute measurements were performed on disks that were cut from the flight samples. The disks were cut by hand using a jeweler's saw (care being taken not to touch the sample surface), and the chips were blown from the surface by use of dry nitrogen. Because the

glass specimens could be positioned in the measuring devices, identical directional- and bidirectional-transmittance measurements were performed both preflight and postflight.

Solar-Reflectance and Solar-Absorptance Measurements

Absolute measurements of solar reflectance were taken in an integrating sphere reflectometer (ref. 1). Reflectance properties of each sample were measured over the wavelength extending from 0.295 to 2.63 micrometers. Solar absorptance was then calculated by numerically integrating the reflectance data over the Johnson solar spectrum (ref. 2) and by subtracting the integral from unity. Relative measurements of solar absorptance were obtained by placing the flight sample at the sample port of a commercial spectroreflectometer (ref. 3) and by placing the standard sample at the reference port. Solar reflectance was then obtained by multiplying the relative reflectance of the flight sample by the absolute reflectance of the standard sample in each of 25 spectral zones (4-percent solar energy bands as defined by Johnson in ref. 2).

Near-normal-emittance absolute measurements were obtained by using the heated cavity absolute reflectometer (ref. 4). Reflectance properties were measured in the 2.0- to 26.0-micrometer spectral region, and the near-normal emittance was calculated by numerically integrating the reflectance data over the 300 K Planckian distribution and by subtracting the integral from unity. Emittance relative measurements were also obtained with an emissometer (ref. 5). Near-normal emittance was calculated by subtracting the reflectance (emissometer meter indication) from unity.

Directional-Transmittance Measurements

Directional transmittance was measured by placing the test sample at the entrance port of the spectroreflectometer (ref. 3). The instrument 100-percent transmittance value was set by running the instrument without a sample in the sample beam. Incident energy transmitted by the specimen was detected either by a photomultiplier tube or by a lead sulfide cell (choice determined by wavelength) mounted at the integrating-sphere wall.

Bidirectional-Transmittance Measurements

Bidirectional transmittance was measured with the bidirectional reflectometer schematically illustrated in figure 8. The optical geometry of the bidirectional measurement is shown in figure 9. The incident-energy beam, the sample, and the detector were arranged so that systematically changing the polar angle θ_2 and the azimuthal angle ϕ_2 made it possible to map the directional distribution of the transmitted radiation over the hemispherical space behind the test surface for a given direction of incidence (θ_1, ϕ_1) and wavelength λ. Polar angle is the angle measured between the surface normal and the incident energy; azimuthal angle is the angle swept when a line in the plane of the sample is rotated counterclockwise about the sample normal until the line is in the plane of the incident beam. The zero angle is arbitrarily set at some recognizable mark on the sample — for example, scratch, bubble, et cetera. The source of radiant energy was a tungsten lamp chopped at 13 hertz, and the detection system was

a commercial monochromator. By chopping the source energy at a constant frequency and by detecting the signal with a tuned alternating-current amplifier, radiant emission from the test specimen and ambient stray light were not detected.

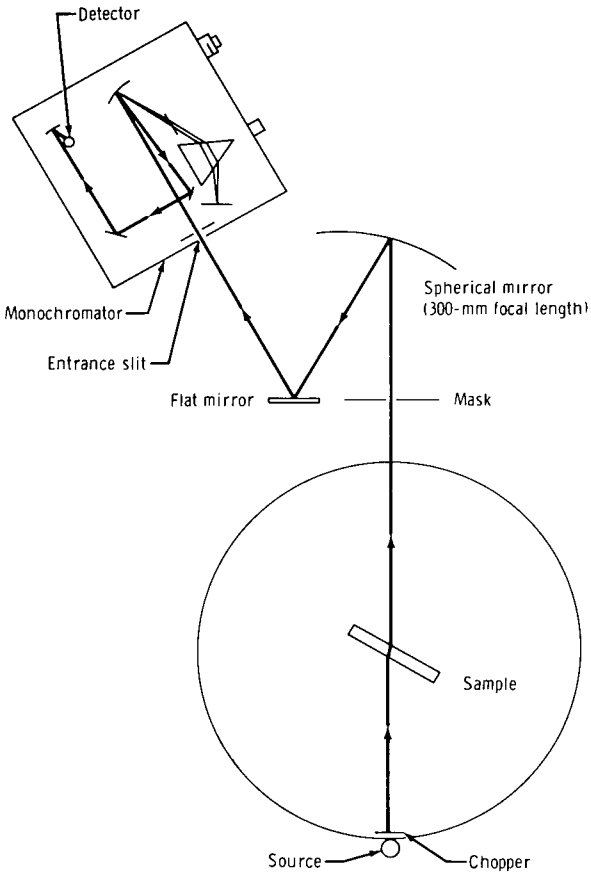

Figure 8. - Schematic representation of the bidirectional reflectometer.

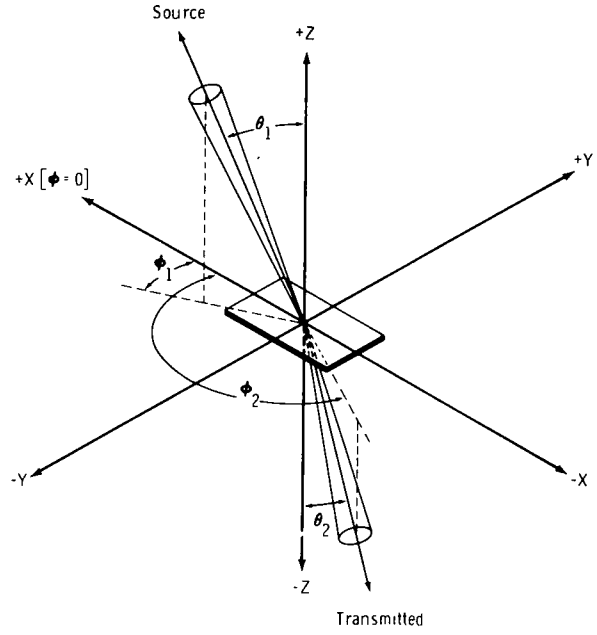

Figure 9. - Optical geometry of the bidirectional reflectometer.

THERMAL-CONTROL-SAMPLE RESULTS

Preflight and postflight numerical results are presented in tables I and II. An indeterminate error exists in the degradation levels because the specific area for postflight measurements may not have been exactly the same area as that measured for preflight. Based on the results of the measurements made on the visibly lightest and darkest areas of the upper left SM sample, this error is small. Representative spectral data are presented in figures 10 to 13.

TABLE I. - SOLAR ABSORPTANCE AND NEAR-NORMAL-EMITTANCE RESULTS

Sample	Type of coating	Solar absorptance, α_s (a)				Near-normal emittance, ϵ_N (a)			
		Integrating sphere reflectometer		Spectroreflectometer		Heated cavity absolute reflectometer		Emissometer	
		Preflight	Postflight	Preflight	Postflight	Preflight	Postflight	Preflight	Postflight
CM	Oxidized silicone monoxide over vacuum-deposited aluminum substrate								
	Flight sample	--	--	0.137	(b)	--	--	0.339	(b)
	Reference 1	0.129	--	--	--	--	--	--	--
	Reference 2	--	--	--	--	0.328	--	.370	--
LM	Chromic-acid anodized aluminum								
	Flight sample 7650	--	--	.678	(c)	--	--	.682	(c)
	Flight sample 7651	--	0.707	.704	0.726	--	--	.728	0.694
	Reference 1	.547	.554	--	--	--	--	--	--
	Reference 2	--	--	--	--	.742	--	.706	.709
SM	Zinc oxide-potassium silicate								
	Flight sample (upper left)	--	[d].291	.195	.282	--	--	.930	.930
		--	[e].232	--	--	--	--	--	--
	Flight sample (upper right)	--	.211	.198	.248	--	--	.927	.925
	Flight sample (lower right)	--	.241	.205	.259	--	0.931	.927	.927
	Reference 1	.164	.166	--	--	--	--	--	--
	Reference 2	--	--	--	--	.920	--	.920	.915
	Titanium dioxide-silicone								
	Flight sample (upper left)	--	.338	.251	.371	--	--	.860	.876
	Flight sample (upper right)	--	.315	.241	.340	--	--	.864	.880
	Flight sample (lower right)	--	.346	.241	.399	--	.880	.864	.869
	Reference 1	.244	.247	--	--	--	--	--	--
	Reference 2	--	--	--	--	.866	--	.868	--
	Reference 2A	--	--	--	--	--	--	.867	.868

[a] Although the accuracy of the measuring instruments does not justify three significant figures, the third figure is retained to indicate trends.

[b] Part not available from Apollo 9 mission.

[c] Designated spare not on Apollo 9 mission.

[d] Darkest area.

[e] Lightest area.

TABLE II. - TRANSMITTANCE MEASURED WITH THE BIDIRECTIONAL SPECTROPHOTOMETER

Window-glass specimen	Polar angle, deg (a)		Wavelength, μm	Transmittance, τ		Azimuth angle, deg	
	θ_1	θ_2		Preflight	Postflight	ϕ_1	ϕ_2
CM	0	0	0.45	0.939	(b)	0	0
	0	0	.65	.950	(b)	0	0
	45	45	.45	.660	(b)	0	180
	45	45	.65	.695	(b)	0	180
LM	0	0	.45	.732	(c)	0	0
	0	0	.65	.930	(c)	0	0
	45	45	.45	.590	(c)	0	180
	45	45	.65	.697	(c)	0	180
LM	0	0	.45	.719	0.692	0	0
	0	0	.65	.939	.925	0	0
	45	45	.45	.557	.510	0	180
	45	45	.65	.744	.745	0	180

[a]As defined in figure 9.

[b]Part not available from Apollo 9 mission.

[c]Designated spare not on Apollo 9 mission.

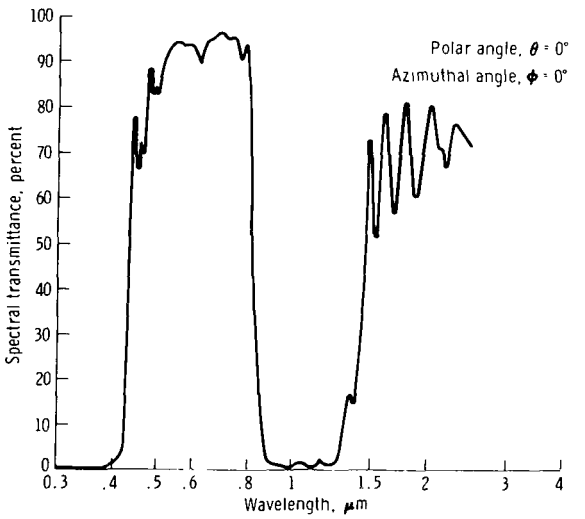

Figure 10. - Preflight and postflight representative spectral data of the LM window specimen on the LM sample.

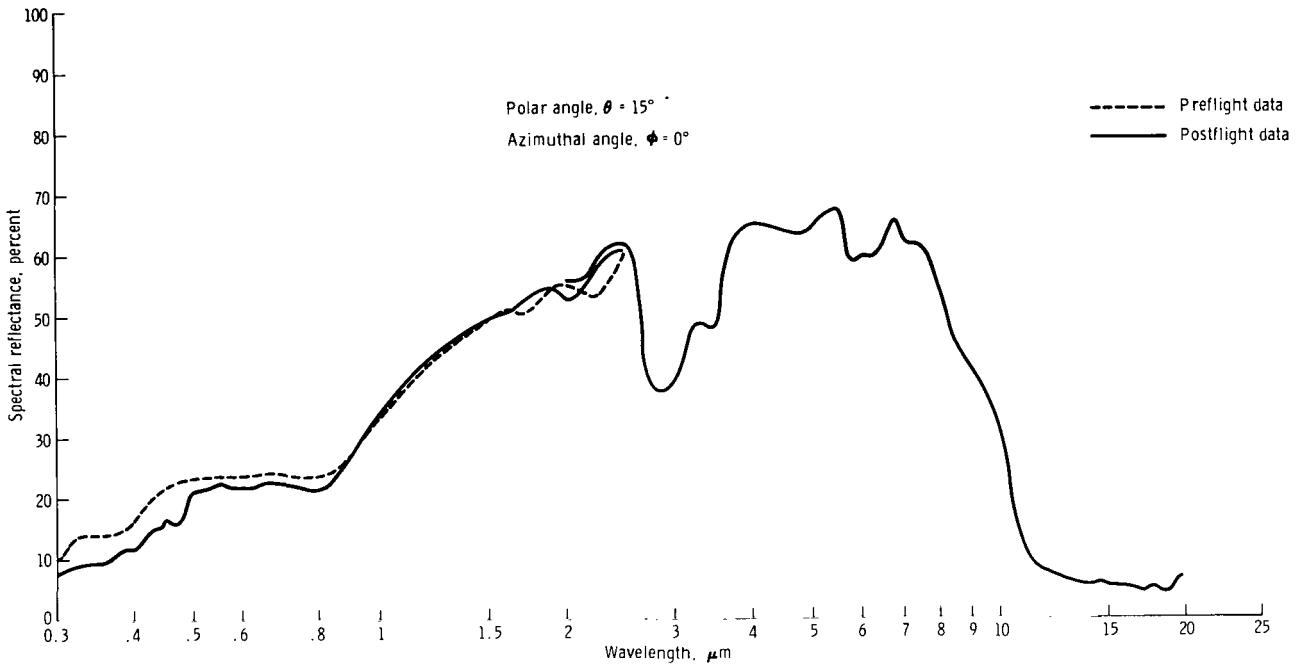

Figure 11. - Preflight and postflight representative spectral data of chromic-acid anodized-aluminum specimen on the LM sample.

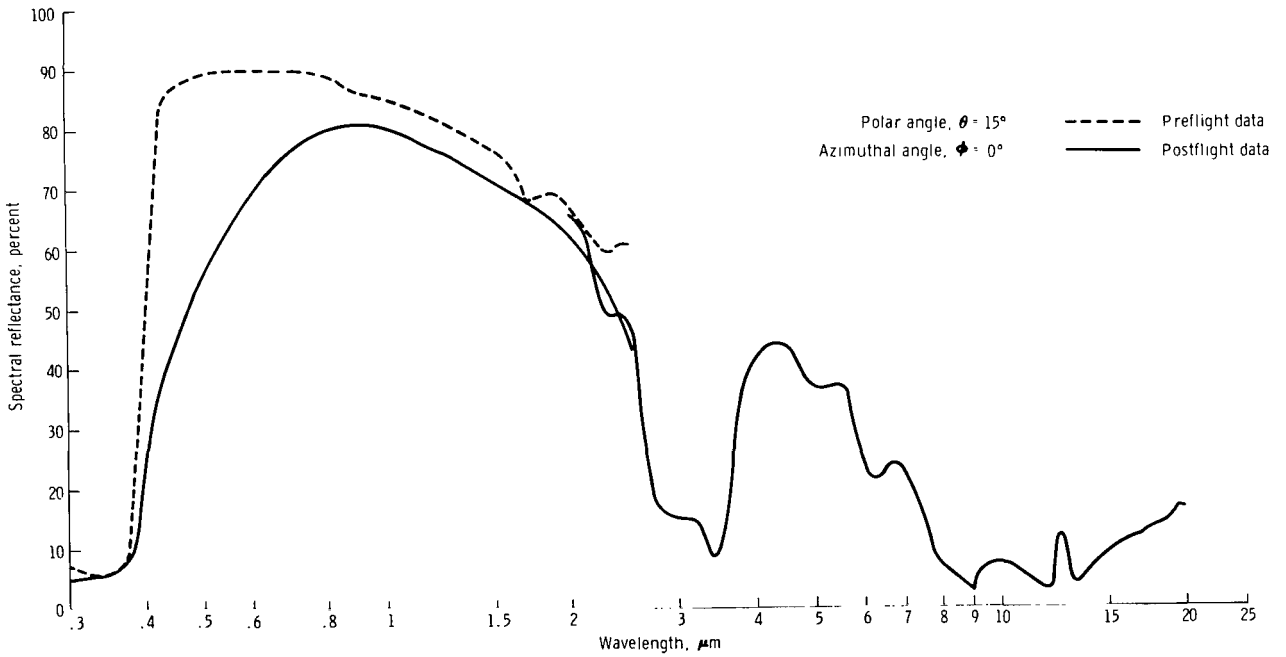

Figure 12. - Preflight and postflight representative spectral data of titanium dioxide-silicone specimen on the SM sample.

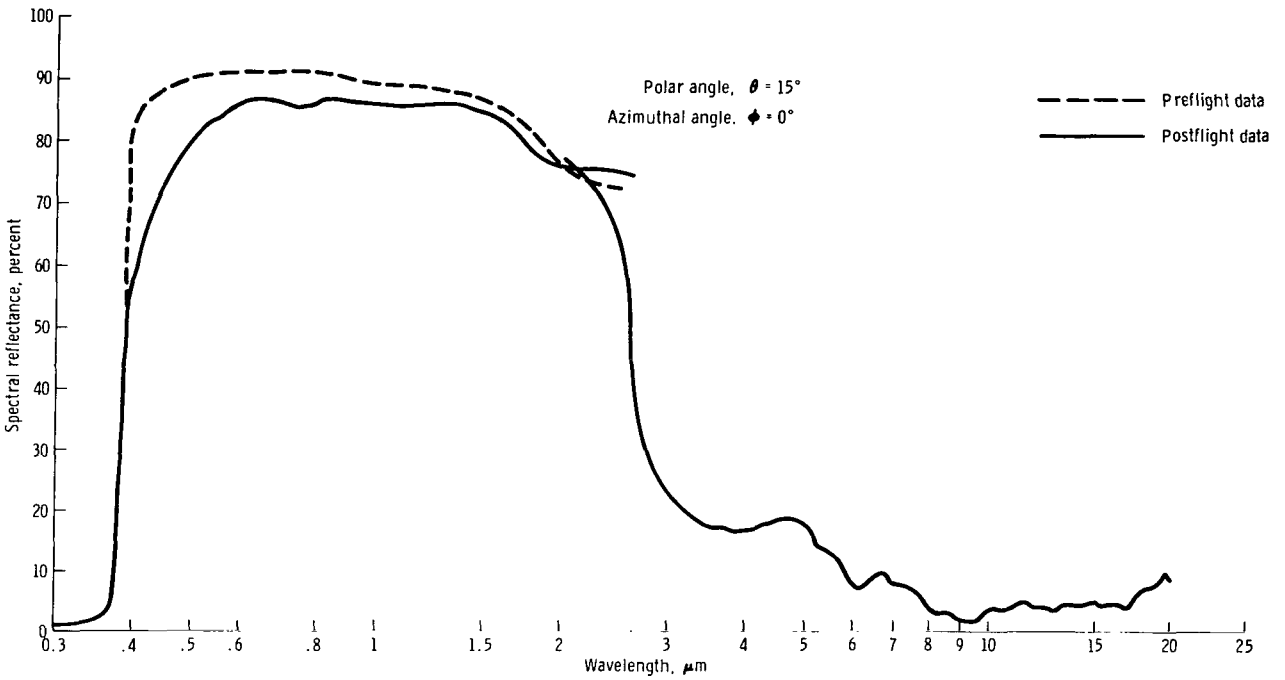

Figure 13. - Preflight and postflight representative spectral data of zinc oxide-potassium silicate specimen on the SM sample.

Lunar Module Sample

Spectral data on the LM window glass are shown in figure 10. The bidirectional spectrophotometric measurements showed a slight decrease in spectral transmittance (table II) between the preflight and postflight measurements. Separate plots are not presented because the postflight measurements so closely match the preflight measurements that the differences are undiscernible when plotted on the same graph.

The spectral data of the chromic-acid anodized-aluminum specimen (fig. 11) showed a slight effect in the short-wavelength region that resulted in an apparent increase in solar absorptance from 0.704 to 0.726. However, an apparent decrease in emittance from 0.728 to 0.694 was also evidenced. It was concluded that virtually no degradation to this control-coating material occurred.

Command Module Sample

As mentioned previously, the CM sample was not in place when the hatch was opened during orbit. The cause for the disappearance of the sample is not known for certain; however, the sample may have been inadvertently removed when the BPC was jettisoned shortly after launch.

Service Module Sample

Representative spectral data of both preflight and postflight measurements of the SM lower right sample are shown in figures 12 and 13. A strong effect in the short-wavelength region with a diminishing effect at increasing wavelengths is obvious for both paint specimens. This apparently indicates a deposited layer of material that is thin enough to affect the short wavelengths but is transparent to the infrared. The fact that the titanium dioxide pigmented silicone (fig. 12) displayed much greater degradation than the zinc oxide pigmented silicate (fig. 13) probably indicates that the surface-adhesive characteristics of the silicone coating caused a subsequent retention of contaminant material that did not adhere well to the silicate material.

A noticeable variation of degradation was observed across the SM samples. The zinc oxide-potassium silicate surface of the upper left flight sample was measured in the lightest and darkest areas, which yielded solar absorptance values of 0.23 and 0.29, respectively. This difference is obvious in a comparison of the reflectance measurements at wavelengths above 0.399 micrometer (table III). This variation probably was the result of local perturbations of the streaming BPC ablation products caused by the sample-tether-attachment fixtures. Noticeable variation in degradation also present on the zinc oxide-potassium silicate surface probably occurred for the same reason. Outgassing of the silicone covering at the tether-attachment fixture (fig. 4) probably added to the overall contamination of the samples. The contamination on the samples was analyzed by emission spectroscopy. The results indicated that contamination from the silicone covering on the tether was present on one of the samples; however, no other contamination could be conclusively identified. X-ray fluorescence and infrared spectroscopy were also used, but no additional contaminants were identified.

The upper left SM sample, alined with the centerline of the RCS engine plume, showed visible signs of contamination from that source. A retention tab on the sample-mounting fixture covered an area approximately 0.3 by 2.5 centimeters on the lower inboard edge of each specimen. This tab deflected the plume so that a shadow area resulted on the specimen. This area was first noticed on the titanium dioxide-silicone surface under oblique lighting conditions (fig. 14). The same shadow pattern was also detected on the zinc oxide-potassium silicate surface under black-light exposure, as shown in figure 15. Because this shadowing effect was evidenced only on the sample that was alined with the RCS engine plume and not on the right-hand samples, visible effects from the RCS engine plume appear only to occur when relatively near the plume.

An area approximately 0.8 centimeter high and 4.4 centimeters long on the lower edge of both hinged plates of the SM samples was found to be darkened (fig. 16). This area was exposed because the Teflon mounting plate was shorter than the SM sample. A cavity actually existed because of the thickness of the mounting plate. This darkening probably resulted from the Saturn I or II solid-propellant retrorocket plumes during staging.

TABLE III. - REFLECTANCE DATA

Slit no.	Wavelength, λ, μm	Dark area, ρ	Light area, ρ	Slit no.	Wavelength, λ, μm	Dark area, ρ	Light area, ρ
1	0.295	0.000	0.000	26	0.722	0.882	0.912
2	.330	.015	.015	27	.743	.885	.915
3	.355	.018	.018	28	.765	.885	.917
4	.377	.083	.075	29	.789	.890	.919
5	.399	.355	.530	30	.814	.895	.920
6	.415	.414	.635	31	.841	.900	.922
7	.430	.465	.677	32	.869	.899	.922
8	.444	.510	.705	33	.899	.901	.922
9	.457	.534	.733	34	.931	.901	.922
10	.470	.570	.757	35	.966	.902	.920
11	.483	.610	.772	36	1.002	.903	.917
12	.496	.645	.792	37	1.044	.903	.917
13	.511	.672	.811	38	1.085	.904	.915
14	.526	.703	.828	39	1.133	.903	.915
15	.540	.724	.840	40	1.185	.900	.915
16	.554	.747	.847	41	1.242	.901	.915
17	.569	.761	.858	42	1.303	.900	.912
18	.584	.773	.867	43	1.381	.896	.908
19	.599	.798	.885	44	1.471	.888	.902
20	.615	.817	.890	45	1.578	.884	.895
21	.631	.835	.890	46	1.714	.864	.878
22	.647	.847	.892	47	1.898	.812	.813
23	.664	.858	.900	48	2.168	.775	.778
24	.683	.865	.905	49	2.632	.142	.427
25	.702	.875	.910	50	3.917	.155	.155
				Total	--	35.451	38.387
				$\bar{\rho}$	--	.709	.768
				α_s	--	.291	.232

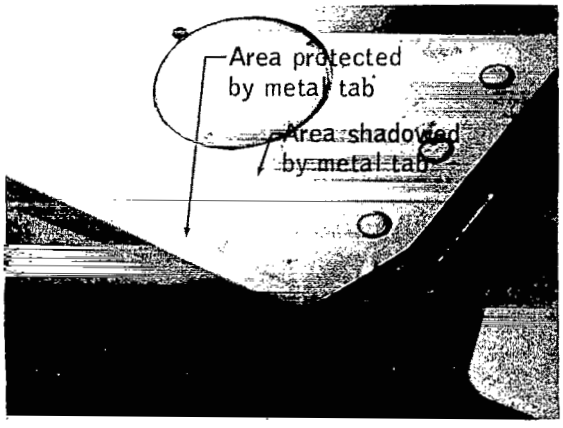

Figure 14.- Plume-impingement shadow effect on titanium dioxide-silicone under oblique lighting conditions.

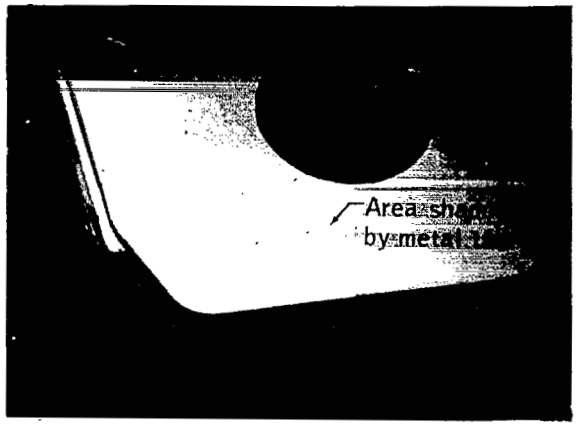

Figure 15.- Plume-impingement shadow effect on zinc oxide-potassium silicate under black-light conditions.

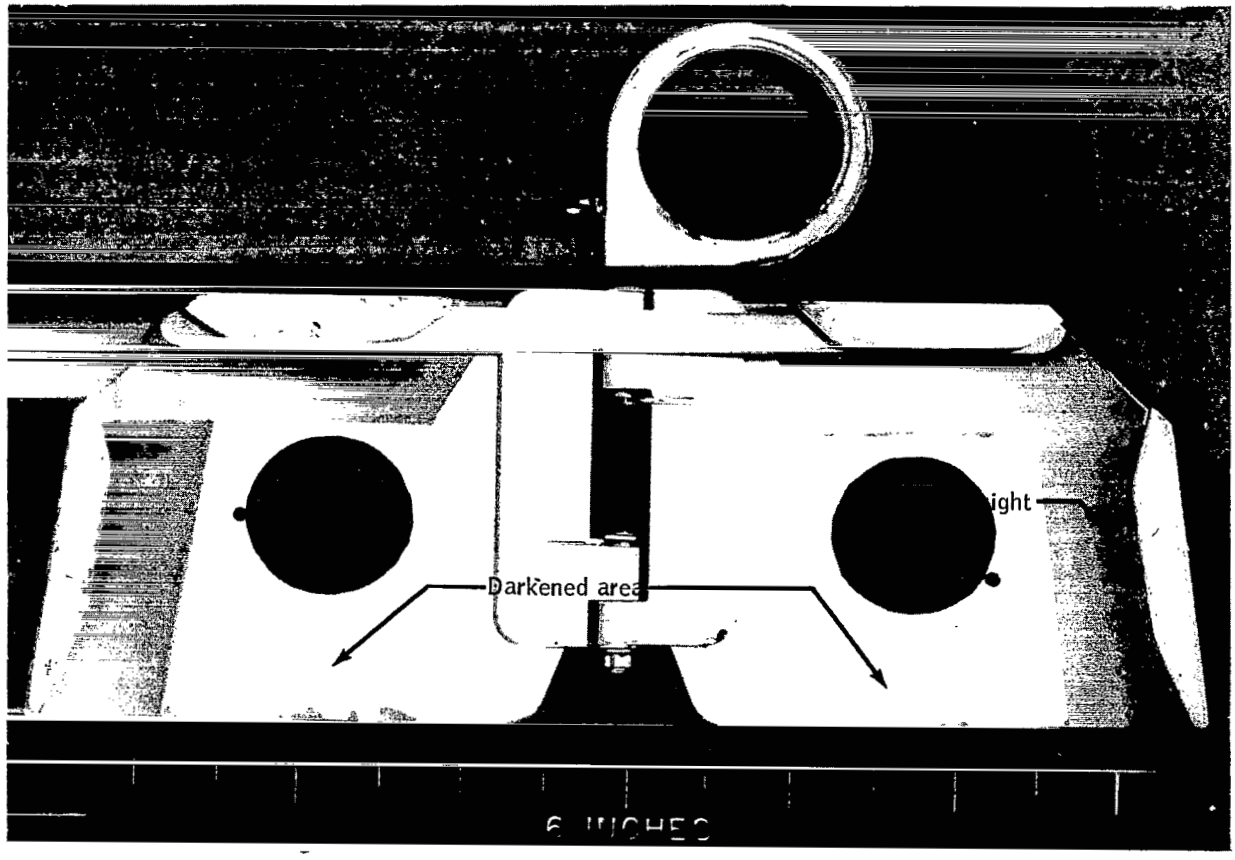

Figure 16. - Degradation on the reverse side of the SM thermal samples.

CONCLUDING REMARKS

The numerical results presented in this report show that the overall degradation levels were well within the design capability of the Apollo spacecraft to perform the lunar-landing missions. Because of proper sample location for maximum combined degradation, the results provided a high confidence level that assured the Apollo design adequacy.

An attempt to evaluate the chemical composition of the degradation constituents was inconclusive. Also, no conclusion was reached concerning which contamination sources provided the majority of contamination. A much more elaborate inflight experiment using several extravehicular-activity or other retrieval methods would be required to evaluate separate contamination sources.

Cumulative firing time of the reaction control system engine impinging on the service module upper left sample was not determined. Because the engine contamination appeared to be a thin transparent film, the overall effects of firing duration for a 200-hour lunar-landing mission would not be significantly worse than the degradation obtained during the 73 hours of the Apollo 9 mission.

National Aeronautics and Space Administration
Manned Spacecraft Center
Houston, Texas, March 24, 1972
914-11-00-00-72

REFERENCES

1. Edwards, D. K.; Grier, J. T.; Nelson, K. E.; and Roddick, R. D.: Integrating Sphere for Imperfectly Diffuse Samples. J. Opt. Soc. Am., vol. 51, no. 11, Nov. 1961, pp. 1279-1288.

2. Johnson, Francis S.: The Solar Constant. J. Meteorol., vol. 11, no. 6, Dec. 1954, pp. 431-439.

3. Cahn, Lee; and Henderson, B. D.: Performance of the Beckman DK Spectrophotometer. J. Opt. Soc. Am., vol. 48, no. 6, June 1958, pp. 380-387.

4. Dunkle, R. V.; Edwards, D. K.; Grier, J. T.; Nelson, K. E.; and Roddick, R. D. Heated Cavity Reflectometer for Angular Reflectance Measurements. Progress in International Research on Thermodynamics and Transport Properties, Joseph F. Masi and Donald H. Tsai, eds., Academic Press (New York), 1962, pp. 541-562.

5. Nelson, K. E.; Bevans, J. T.; and Luedke, E. E.: A Device for the Rapid Measurement of Total Emittance. J. Spacecraft Rockets, vol. 3, no. 5, May 1966, pp. 758-760.

NASA-Langley, 1972 —— 31 S-314

"The aeronautical and space activities of the United States shall be conducted so as to contribute . . . to the expansion of human knowledge of phenomena in the atmosphere and space. The Administration shall provide for the widest practicable and appropriate dissemination of information concerning its activities and the results thereof."

—NATIONAL AERONAUTICS AND SPACE ACT OF 1958

NASA SCIENTIFIC AND TECHNICAL PUBLICATIONS

TECHNICAL REPORTS: Scientific and technical information considered important, complete, and a lasting contribution to existing knowledge.

TECHNICAL NOTES: Information less broad in scope but nevertheless of importance as a contribution to existing knowledge.

TECHNICAL MEMORANDUMS: Information receiving limited distribution because of preliminary data, security classification, or other reasons.

CONTRACTOR REPORTS: Scientific and technical information generated under a NASA contract or grant and considered an important contribution to existing knowledge.

TECHNICAL TRANSLATIONS: Information published in a foreign language considered to merit NASA distribution in English.

SPECIAL PUBLICATIONS: Information derived from or of value to NASA activities. Publications include conference proceedings, monographs, data compilations, handbooks, sourcebooks, and special bibliographies.

TECHNOLOGY UTILIZATION PUBLICATIONS: Information on technology used by NASA that may be of particular interest in commercial and other non-aerospace applications. Publications include Tech Briefs, Technology Utilization Reports and Technology Surveys.

Details on the availability of these publications may be obtained from:

SCIENTIFIC AND TECHNICAL INFORMATION OFFICE

NATIONAL AERONAUTICS AND SPACE ADMINISTRATION

Washington, D.C. 20546